Dissociative recombination of rotationally cold H_3^+

B. J. McCall,* A. J. Huneycutt,† and R. J. Saykally
Department of Chemistry, University of California at Berkeley, Berkeley, California 94720, USA

N. Djuric‡ and G. H. Dunn
JILA, University of Colorado and National Institute of Standards and Technology, Boulder, Colorado 80309-0440, USA

J. Semaniak and O. Novotny§
Institute of Physics, Swietokrzyska Academy, 25 406 Kielce, Poland

A. Al-Khalili, A. Ehlerding, F. Hellberg, S. Kalhori, A. Neau, and R. D. Thomas
Department of Physics, AlbaNova, Stockholm University S-106 91 Stockholm, Sweden

A. Paal and F. Österdahl
Manne Siegbahn Laboratory, Stockholm University, S-104 05 Stockholm, Sweden

M. Larsson
Department of Physics, AlbaNova, Stockholm University S-106 91 Stockholm, Sweden
(Received 3 March 2004; published 30 November 2004)

This paper presents the first dissociative recombination (DR) measurement of electrons with rotationally and vibrationally cold H_3^+ ions. A dc discharge pinhole supersonic jet source was developed and characterized using infrared cavity ringdown spectroscopy before installation on the CRYRING ion storage ring for the DR measurements. Rotational state distributions ($T_{rot} \sim 30$ K) produced using the source were comparable to those in the diffuse interstellar medium. Our measurement of the electron energy dependence of the DR cross section showed resonances not clearly seen in experiments using rotationally hot ions, and allowed calculation of the thermal DR rate coefficient for ions at interstellar temperatures, $\alpha_{DR}(23\ \mathrm{K}) = 2.6 \times 10^{-7}\ \mathrm{cm}^3\ \mathrm{s}^{-1}$. This value is in general agreement with recent theoretical predictions by Kokoouline and Greene [Phys. Rev. A **68**, 012703 (2003)]. The branching fractions of the two breakup channels, $H+H+H$ and $H+H_2$, have also been measured for rotationally and vibrationally cold H_3^+.

DOI: 10.1103/PhysRevA.70.052716 PACS number(s): 34.80.Lx, 34.80.Gs, 39.10.+j, 33.20.Ea

I. INTRODUCTION

The simplest polyatomic ion, H_3^+, has provided a constant intellectual challenge to experimentalists and theoreticians since its discovery by Thomson in 1911 [1]. Its importance as a dominant species in hydrogen plasmas was recognized early [2]. Upon ionization of molecular hydrogen, H_2^+ reacts readily with the more abundant neutral H_2 in the exothermic (1.7 eV) reaction [3] $H_2 + H_2^+ \rightarrow H_3^+ + H$. The large cross section [4] and high exothermicity [5] of this reaction, together with the widespread abundance of H_2, led Martin *et al.* in 1961 to postulate that H_3^+ could be present in interstellar space [6]. In 1973, Watson [7] and, independently, Herbst and Klemperer [8], suggested that H_3^+ could initiate ion-neutral reactions that would lead to the formation of the many molecules observed in dense interstellar clouds by radio and millimeter wave astronomy. These ideas provided the groundwork for understanding dense cloud chemistry through the proton transfer reaction $H_3^+ + X \rightarrow HX^+ + H_2$, where X can be almost any atom or molecule. The high reactivity of H_3^+ is due to the relatively low proton affinity (4.5 eV) of molecular hydrogen, and the associated rapid proton transfer distinguishes it as the "universal protonator."

Interstellar H_3^+ was first detected spectroscopically in 1996 by Geballe and Oka [9] in the dense cloud sources W33A and AFGL 2136. Subsequently, a survey [10] of dense molecular clouds ($n \sim 10^3$–$10^5\ \mathrm{cm}^{-3}$) demonstrated the use of H_3^+ as a probe of the path length, density, and temperature of these clouds, and confirmed the general picture of ion-neutral chemistry. In contrast, the discovery of H_3^+ in diffuse interstellar clouds ($n \sim 10$–$10^3\ \mathrm{cm}^{-3}$) by McCall *et al.* in 1998 [11] was completely unexpected. Similar column densities were observed for both environments, which was quite surprising, given the high electron concentration and the efficiency of DR in the diffuse interstellar medium. The understanding of diffuse cloud chemistry to that point gave esti-

*Present address: Department of Chemistry, School of Chemical Sciences, University of Illinois at Urbana-Champaign, 600 South Mathews Avenue, Urbana, IL 61801, USA.

†Present address: Aerospace Corporation, Los Angeles, CA 90009-2957.

‡Present address: Jet Propulsion Laboratory, California Institute of Technology, Pasadena, CA 91109-8099, USA.

§Also at Department of Electronics and Vacuum Physics, Faculty of Mathematics and Physics, Charles University Prague V Holesovickach, Prague 8, Czech Republic.

mates of the H_3^+ number density that were far too low to account for the observed column density [12], prompting many to speculate that the adopted laboratory value ($\sim 2 \times 10^{-7}$ cm^3 s^{-1}) of the DR rate was incorrect, or inapplicable under interstellar conditions.

In fact, laboratory determinations of the H_3^+ DR rate have been controversial for some time, as has been reviewed by Oka [13], by Larsson [14], and by Plasil *et al.* [15] The earliest measurements of the DR rate in the early 1950s gave values of a few $\times 10^{-6}$ cm^3 s^{-1} at 300 K, whereas a series of measurements in the 1970s using different techniques (e.g., Leu *et al.* [16]) generally agreed on a thermal DR rate coefficient (α_{DR}) of $\sim 2 \times 10^{-7}$ cm^3 s^{-1}. This agreement persisted until 1984, when Smith and Adams [17] reported that their flowing afterglow Langmuir probe (FALP) measurements did not show *any* DR of H_3^+, with an upper limit of $\alpha_{DR} < 2 \times 10^{-8}$ cm^3 s^{-1}. In 1989, Adams and Smith [18] lowered their upper limit to 10^{-11} cm^3 s^{-1}, and much of the community accepted a low value of α_{DR}—even the models of diffuse interstellar clouds were changed [19], predicting large quantities of H_3^+ due to the presumed inefficiency of its destruction.

The tide turned back to high values of the DR rate in 1990, when Amano [20,21] utilized infrared absorption spectroscopy to directly probe the loss of H_3^+ in its lowest vibrational level, finding a (rotationally averaged) value of $\alpha_{DR} \sim 1.8 \times 10^{-7}$ cm^3 s^{-1} at 273 K. Since that time, there has been about a one order of magnitude range of values from FALP measurements, in the range $0.2-2 \times 10^{-7}$ cm^3 s^{-1}. In 1994, the first measurement of H_3^+ DR using the storage ring technique was made at CRYRING [22] (Stockholm, Sweden), and yielded a value of 1.15×10^{-7} cm^3 s^{-1} at 300 K. Subsequent storage ring experiments at TARN II [23] (Tokyo, Japan) and ASTRID [24] (Aarhus, Denmark) agreed with the CRYRING results within the combined error bars. While the storage ring measurements are in general agreement with the upper end of the FALP results, a new controversy has erupted as a result of recent stationary afterglow measurements [25] that claim an unusual pressure dependence of the DR rate, set an upper limit of 4×10^{-9} cm^3 s^{-1}, and are in clear disagreement with all other experiments. The reason(s) for the disagreement among the FALP results, and between the stationary afterglow results and the other measurements, are still very much unclear. Nevertheless, the recent consensus is that the higher value reestablished by Amano and confirmed by all the storage ring measurements (as well as some of the FALP studies) is likely to be correct.

A major advantage of storage ring experiments over other techniques is that the long storage times involved ensure that ions have time to relax to the lowest vibrational level before measurements are performed. Recent experiments [26] using the Coulomb explosion imaging technique at the Test Storage Ring (Heidelberg, Germany) have confirmed that conventional (hot) plasma sources initially produce a significant fraction of vibrationally excited H_3^+, but that a storage time exceeding 2 s is sufficient to relax the ions into the ground vibrational state. However, these experiments [27] also demonstrated that the H_3^+ ions retained their initial (high) rotational excitation for storage times up to 40 seconds, as expected for a molecule with no permanent dipole moment. Recent experiments at CRYRING [28] showed a dependence of DR rates on hollow cathode source conditions and ion storage times, suggesting a possible variation of the DR cross-section with the rotational level of H_3^+. Similar observations have been made for D_2H^+ by Lammich *et al.* [29] and Wolf *et al.* [30] using the Test Storage Ring.

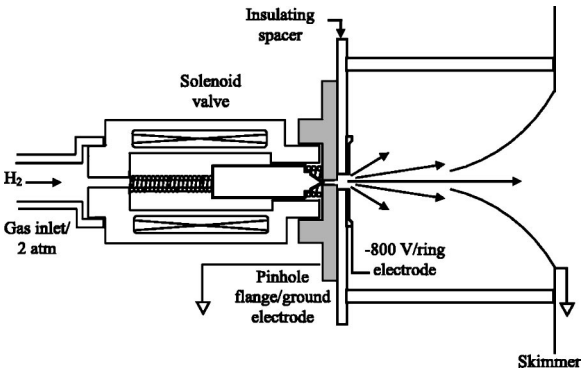

FIG. 1. Cross section of the Berkeley cold-ion pinhole source used to produce rotationally cold H_3^+. The ground electrode and entire source assembly is floated at a voltage of +30 kV on the CRYRING endstation. The values of the H_2 gas pressure and dc discharge voltage were typical of those used during DR experiments (see text). Figure is not to scale.

These observations, coupled with the importance of the DR process in the interstellar medium, prompted us to undertake the present study of H_3^+ DR using a source that produces rotationally cold ions, with a distribution similar to that in the interstellar medium. A preliminary report on the results of this experiment has appeared elsewhere [31]; in this paper we describe the experiment and data analysis in more detail.

II. EXPERIMENT

A. Ion source and spectroscopic characterization

The key advance in the present experiment was the development of a supersonic expansion ion source that produces rotationally cold H_3^+ ions. This source was developed and spectroscopically characterized at the University of California, Berkeley, before being used for DR measurements at the CRYRING ion storage ring at the Manne Siegbahn Laboratory in Stockholm, Sweden. As can be seen in the cross section of the source in Fig. 1, the source consists of a 500 μm circular pinhole through which hydrogen gas at a pressure of ~ 2 atm is expanded into a chamber evacuated by a high throughput pumping system. A solenoid valve (General Valve, Series 9) actuates the poppet, allowing the gas to be pulsed, with typically a ~ 400 μs pulse gate width and a repetition of <1 Hz (at CRYRING) or 50 Hz (at Berkeley). Performance of the source was not affected for pulse lengths from 350 μs to at least several milliseconds. The pulse length was limited by the maximum safe duty cycle ($\sim 1\%$) of the source driver used at CRYRING. The short pulse limit reflected the turn-on time of the gas pulse, as poor shot-to-

shot stability in gas throughput (as monitored by peak chamber pressure fluctuations) was observed for pulse widths below ~300 μs. The lower time limit for stable operation was a function of the driving voltage on the solenoid valve; a value of 300 V seemed to provide good valve performance for the pulse lengths used in these studies. As the gas expands through the pinhole, it is ionized in a discharge maintained by a dc potential ($\geqslant$450 V) maintained between the pinhole flange plate and a low-profile ring electrode. A grounded skimmer is also mounted downstream, centered on the expansion axis, in order to reduce the off-axis ion current emitted from the source without lowering the (on-axis) current delivered to the CRYRING storage ring.

The rotational state distribution of the H_3^+ ions was determined using direct absorption spectroscopy in the region just beyond the ring electrode and upstream of the skimmer. The cavity ringdown spectrometer employed for the absorption measurements has been explained in detail elsewhere [32,33] and will be described here only briefly. A 50 Hz Nd:YAG (Spectra Physics 290-50, 500 mJ/pulse at 532 nm) pumped dye laser (Lambda Physik FL3002E) was used to generate tunable pulsed visible radiation which was then shifted by three Stokes shifts in a multipass cell containing 14 atm of H_2 gas to produce up to 0.5 mJ/pulse of tunable IR light. The dye laser was operated with an intracavity etalon, which narrowed the laser emission bandwidth from 0.2 cm^{-1} to 0.04 cm^{-1}. The Stokes-shifted radiation was filtered to pass only the desired third-Stokes light, which was subsequently injected into a cavity formed by two ringdown supermirrors ($R \sim 0.9998$). The cavity output was focused onto a liquid N_2-cooled InSb detector (Infrared Associates, $D^* \sim 10^{10}$ cm $Hz^{1/2}$ W^{-1}) and the signal was amplified, digitized, averaged (40 ringdown traces per wavelength point), and fit to a first-order exponential decay. The optical transit time of our cavity divided by the decay constant determined from a single exponential fit of the detector signal gave the per-pass total cavity loss at that wavelength. Typical values for the per-pass loss of an empty cavity at the maximum reflectivity of our 3.3 μm supermirrors were on the order of 140 ppm.

Absorption spectra of the $R(1,0)$ and the $R(1,1)^u$ transitions of H_3^+ near 2726 cm^{-1} were obtained under a variety of source conditions to monitor the rotational distribution. This "doublet" of lines serves as an effective probe of the rotational temperature (assuming the ortho and para spin modifications are thermalized), as it arises from the two lowest rotational levels, which differ in energy by only about 23 cm^{-1}. Typical spectra are shown in Fig. 2, and display rotational temperatures similar to that seen in diffuse clouds [31]. Because we were not equipped to perform spectroscopy during the DR experiments in Stockholm, we obtained spectra in Berkeley over a wide range of parameters such as source-gas pressure and composition, pulse length, plasma discharge voltage, and the relative timing between the gas pulse and discharge pulse. In general, we found that the rotational temperature was not very sensitive to these parameters, staying between 20–60 K under a wide range of source conditions.

A small variation in the rotational temperature was observed as the dc discharge voltage was raised from the

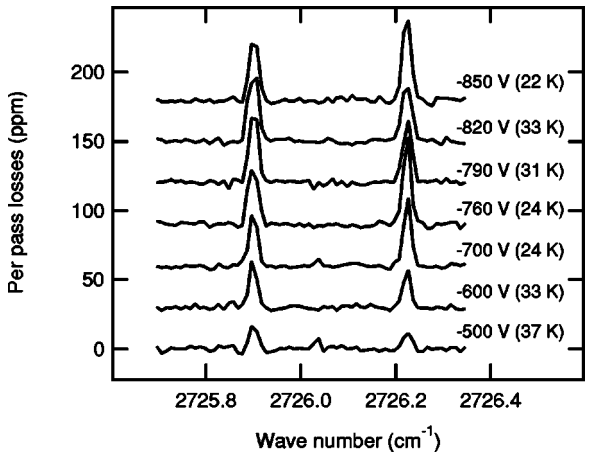

FIG. 2. Cavity ringdown spectra of the $R(1,0)$ and $R(1,1)^u$ lines of H_3^+ as a function of dc discharge voltage. Temperatures (listed in parentheses) were determined from the ratio of the integrated areas of the two peaks. Spectra have been background subtracted, and shifted vertically for clarity.

detection-threshold voltage. Figure 2 illustrates the spectral differences as the discharge voltage was increased from −500 V to −850 V. Little difference was found between the spectra, with only slight variations in temperature between 22 K and 37 K. Most of the CRYRING experiments were done using −800 V discharge voltage, which was well within the range of low temperature operation. The most significant difference in the spectra recorded at different discharge voltages was the number density of ions, which rose from $\sim 2.6 \times 10^{10}$ cm^{-3} at −500 V to $\sim 1.1 \times 10^{11}$ cm^{-3} at −760 V, and did not change much at higher voltages. These number densities represent higher ion currents than are needed for the storage ring experiments.

Other factors investigated, such as the dilution of H_2 in He, were found to reduce the number density of H_3^+ without affecting the rotational temperature. Varying the source pressure (pure H_2) from 1–5 atm had no noticeable effect on the rotational temperature. The cavity ringdown spectra obtained at the beginning, middle, and end of the discharge pulse were all similar, indicating that cold ions are produced along the entire temporal length of the discharge. Similarly, changing the position in time of the discharge pulse (~100 μs width) along the length of the gas pulse (~400 μs width) had no effect on the spectrum.

By translating the ion source with respect to the axis of the laser beam, we obtained cavity ringdown spectra at various chords through the (presumably) axially symmetric plasma. These measurements showed that the H_3^+ rotational temperature was lowest in the middle of the plasma, and higher above or below the center of the pinhole. This suggests that the ions formed in the center of the expansion are colder than the ions formed further away (radially) from the expansion axis. Because the cavity ringdown spectroscopy samples both the central (very cold) ions and the surrounding (warmer) ions, it is likely that the temperatures we report (20–60 K) represent an upper limit to the temperature of the on-axis ions.

Throughout our source characterization, high rotational temperatures were only observed when using a deformed

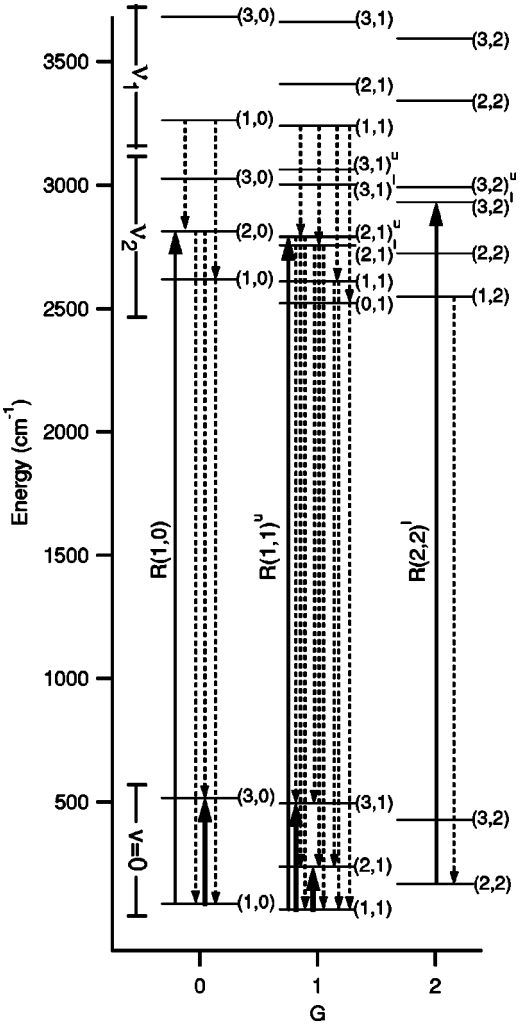

FIG. 3. A simplified energy level diagram of H_3^+. Energy levels are plotted versus the quantum number $G \equiv |k-\ell|$, where k is the projection of J onto the molecular symmetry axis and ℓ is the vibrational angular momentum associated with the ν_2 mode. Each level is labeled on the right as (J,G), with superscript u and l to indicate the upper and lower levels of doublets. A complete explanation of the notation and energy level structure of H_3^+ can be found in [34]. The infrared transitions used are shown by upward-going thin arrows, and the allowed electron-impact excitation transitions are shown as thick arrows. The downward-going dashed arrows indicate the radiative relaxation pathways for the small fraction of ions produced in vibrationally excited (yet rotationally cold) states.

poppet that lacked the smooth conical tip usually used for pinhole molecular beam applications. In such cases the rotational temperature of the ions was observed to be >100 K. At these higher rotational temperatures, it was possible to observe the $R(2,2)^l$ transition of H_3^+ at 2762 cm^{-1}, which arises from the next-highest rotational level (see Fig. 3). When it was detectable, the intensity of the $R(2,2)^l$ line was consistent with the rotational temperature determined from the doublet at 2726 cm^{-1}. At lower temperatures, the $R(2,2)^l$ transition was below our detection limit, which limited the abundance of the (2,2) level to a maximum of about 10% of that of the (1,1) level, corresponding to a temperature of <50 K.

The Teflon poppets used in our experiments were found to be subject to deformation and high temperature ion production after extended usage, due to the softness of the material. To check that the poppet had not deformed during the course of the DR measurements, we returned the source to Berkeley immediately after the storage ring experiments and obtained the spectra illustrated in Fig. 2, confirming that the rotational temperature of the ions was very low. Subsequently, we discovered that poppets made from harder materials, such as Kel-F, will produce low temperature ions with much longer operational lifetimes, but that leakage is somewhat of a problem with these harder materials.

B. Ion injection and CRYRING configuration

The heavy-ion storage ring CRYRING at the Manne Siegbahn Laboratory in Stockholm, Sweden was used to measure the dissociative recombination rate of H_3^+ ions produced at low rotational temperature with the Berkeley ion source. Detailed descriptions of the apparatus, theory, and the standard data analysis for dissociative recombination measurements are available [35], so only a brief description will be given here.

The Berkeley ion source was floated at a potential of 30 kV. After extraction, the ions were mass selected by a dipole magnet. The mass selected ion beam was accelerated to 300 keV/amu in a radiofrequency quadrupole (RFQ), and then injected into CRYRING, which is a roughly circular ion storage ring comprised of twelve dipole bending magnets, and thus, twelve straight sections, which combine to give a path length of approximately 51.6 m. An accelerator, beam diagnostic equipment, the electron cooler, and experiments occupy the straight sections around the ring. Once the beam is stored, the electron cooler is the most important component of the DR experiment. In this experiment, the ions were accelerated to 12.1 MeV immediately after injection into the ring.

The electron cooler supplies the nearly monoenergetic beam of electrons with which the ions react in the DR process. It consists of a 4 mm cathode electron gun housed in a superconducting solenoid, guiding solenoids, electron beam steering toroids, and an electron collector. Electrons are cooled from an initial isotropic energy spread of ~ 100 meV (1000 K) to a longitudinal spread of 0.1 meV (1 K) by acceleration in the electron beam direction. Transverse energy spread is then reduced by adiabatic expansion in the presence of a reducing magnetic field along the beam path, leading to a transverse energy spread of $\sim 2 \pm 0.5$ meV (20 ± 5 K). An electron beam of 35.5 mA was used in the present experiment.

Toroidal magnets merge the electron beam collinearly with the ion beam along a straight section between dipole magnets. In the region where the ion and electron beams are overlapped, the ion beam is altered by the presence of the field of the electrons. One result is that a Coulomb attraction imposes a drag force on the ions. Through this interaction the velocity spread in the ion beam is reduced and the phase-

space volume of the ion beam decreases. Because this process effectively "cools" the ion beam's translational temperature, the apparatus is called the electron cooler. When the electron velocity is matched to the velocity of the ions, the interaction is at its greatest, and heat transfer from the ion beam to the electrons is at its maximum. Thus, when the electron cooler is operating with 0 eV relative energy between the electrons and ions, the beam is "cooling" most efficiently.

In addition to this cooling process, the ions can also undergo DR in the electron cooler, producing neutral fragments. These neutral fragments are not affected by the dipole bending magnets, and their velocity distribution is determined by the energetics of the fragmentation process. Generally the fragments travel with acceptably small divergence tangential to the ring, where they are detected using a surface barrier detector (SBD) that is sensitive to the total energy impinging upon it. Since all fragments from a single DR event arrive at the detector simultaneously (given the bandwidth of detection), the SBD acts as a counter for DR events. Care is taken to keep the ion current low enough not to saturate the SBD (count rate <20 kcps) when the beam is cooling and the recombination events are at their maximum.

In addition to DR in the electron cooler, the ions are also destroyed by collisions with residual gas molecules. Neutral particles from such collisions in the straight section hosting the electron cooler will impinge on the SBD and give rise to counts at 2/3 and 1/3 of the full beam energy, corresponding to one or two hydrogen atoms. The high beam energy makes production of three hydrogen atoms very unlikely since this would require electron capture of H_3^+ ions from residual gas molecules, a process which has a very small cross section at MeV energies. Since collisions with residual gas molecules occur along the entire ring with a frequency directly proportional to the number of stored ions, a different straight section of the ring has a scintillation detector mounted in the 0° direction after the dipole magnet, which provides a convenient beam intensity monitor.

C. CRYRING experimental scheme

The energy dependence of the DR cross section (σ) is given in terms of the average electron energy relative to that of the ions, denoted E_d, where d stands for detuning. The detuning energy is related to the detuning velocity by $E_d = (m_e/2)v_d^2$, where v_d is the average velocity of the electrons with respect to the ions. The laboratory electron energy E_e (in eV) is determined from the effective electron cooler cathode voltage U_e (in V) by the relation $eU_e = E_e$. The effective cathode voltage is equal to the power supply output voltage compensated for the voltage drop across the electron gun cathode and the space charge potential created by the uniform distribution of electrons in the electron beam. The electric field within the electron beam is proportional to the distance from the center of the beam, but since the ion beam is translationally cooled, and hence has a diameter of less than 1 mm, the effective cathode voltage relevant to the center of the electron beam is used. The detuning energy is then given by

$$E_d = (\sqrt{E_e} - \sqrt{E_{e\text{-}cool}})^2, \tag{1}$$

where $E_{e\text{-}cool}$ is the laboratory energy at which the electrons have the same velocity as the ions. Since the space charge correction cannot be calculated exactly because of the presence of slow, positively charged ions (H_2^+ from electron impact ionization of background gas) in the electron beam, which to some extent offsets the electron space charge potential, the Schottky noise power spectrum of the circulating ion beam was measured and used to determine $E_{e\text{-}cool}$. The Schottky noise is the ac component of the circulating beam, which arises from statistical fluctuations of the particle distribution. It can be picked up by probes near the beam and amplified by low-noise amplifiers. For the 12.1 MeV H_3^+ beam, the Schottky frequency was determined to be 539730 Hz.

In order to determine the cross section as a function of E_d, the electron energy (i.e., the electron cooler voltage) was ramped and the neutral particle count rates were recorded as a function of time during these ramps. The electron energy was ramped symmetrically around the cooling energy in order to facilitate the determination of the energy scale. The cooling energy is readily determined from the fact that the production of neutral particles has a maximum at this energy. Figure 4 shows the ramping schemes used in the experiment.

The rate coefficient (α_{DR}), which is the velocity-weighted cross section (averaged over the velocity distribution of the electrons in the cooler), for DR at a particular electron energy is calculated by [36]

$$\alpha_{\mathrm{DR}}(E_d) = R_b \frac{C}{n_e l_{ec}} \frac{N_{\mathrm{DR}}}{N_B}, \tag{2}$$

where N_B is the background counts measured in the scintillation detector, R_b is the destruction rate per ion and per unit time in the straight section containing the scintillation detector, C is the ring circumference, n_e is the electron density, l_{ec} is the length of the electron cooler, and N_{DR} is the number of DR events measured with a surface barrier detector positioned after the electron cooler. Absolute values for the rate coefficients are possible because the R_b term includes the total ion current (I_i)

$$R_b = \frac{v_i q C_{\mathrm{ref}}}{C I_i}, \tag{3}$$

where q is the elementary charge, v_i is the ion velocity and $C_{ref} = d(N_B)/dt$ is the count rate measured by the scintillation detector. The advantage with this procedure is that the ion current can be related to R_b by an independent measurement where I_i can be maximized without concern for the SBD, which is blocked during this measurement. The ion current was measured by a Bergoz Beam Charge Monitor with Continuous Averaging (BCM-CA) and an Integrating Current Transformer (ICT) [37] to give a calibration factor for the neutral particle scintillation detector. The circulating ion current was measured to be 310 nA.

Corrections for the toroidal regions of the electron cooler are then included. In these regions the ion and electron beams are not collinear, and the relative velocity between

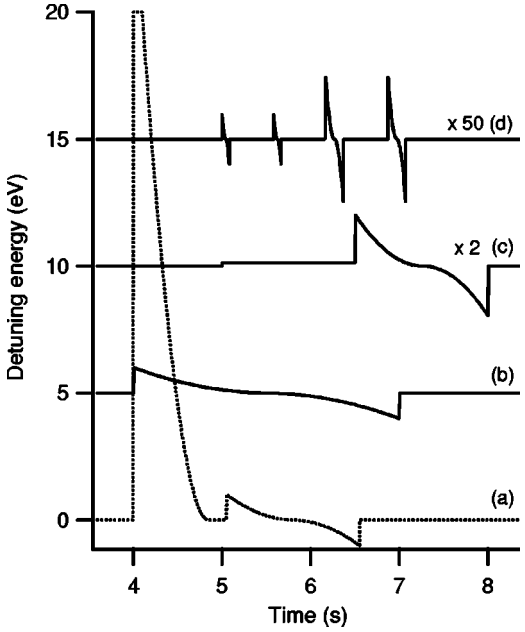

FIG. 4. Ramping schemes used for DR measurements. Ramp (a), shown by a dotted line, spans detuning energies from 0 to 20 eV. Ramp (b) covers detuning energies from +1 to −1 eV. In ramp (c), the ion beam was heated for 1.5 s by exposing it to electrons just above the threshold for the $(3,0)\leftarrow(1,0)$ transition, before making DR measurements at detuning energies from +1 to −1 eV. In ramp (d), low energy DR measurements were performed without exposing the ion beam to electrons above the $(2,1)\leftarrow(1,1)$ threshold (for $t<6$ s) or the $(3,0)\leftarrow(1,0)$ threshold (for $t<6$ s), as discussed in Sec. IV B. Ramps (b)–(d) have been offset vertically for clarity, and ramps (c) and (d) have been vertically expanded to show detail. In all experiments, the ion beam was stored for at least four seconds ($t=0$ corresponds to injection into the ring).

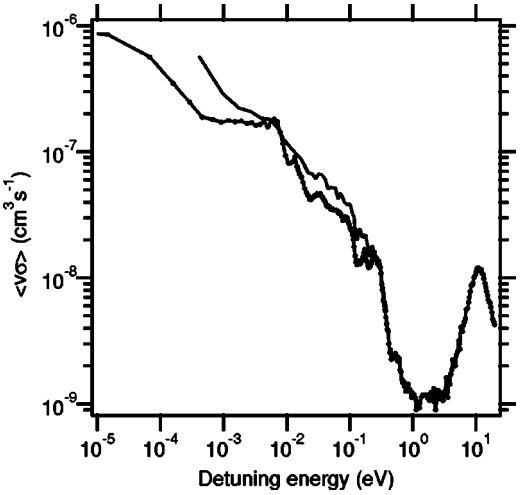

FIG. 5. Measured dissociative recombination rate as a function of detuning energy. The curve with dots is the data obtained in this work using the Berkeley supersonic expansion ion source. For comparison, the curve without dots is from a run using the JIMIS hollow cathode source, as reported in [28].

electrons and ions is greater than in the straight portion of the electron cooler. The straight section is 85 cm, and the distance between the toroidal magnets at each end of the cooler is 110 cm. The electron and ion beams are no longer collinear outside the 85 cm straight section, which implies that with increasing beam angle $\theta(x)$, the collision energy between ions and electrons increases rapidly. The correction procedure was based on the beam angle $\theta(x)$ as determined from magnetic field measurements. The correction to the rate coefficient is applied iteratively according to the procedure outlined by Lampert *et al.* [38]. Because the correction basically involves subtracting two large numbers from one other, it is very sensitively dependent on the exact conditions in the toroidal regions. The results in the 0.5–5 eV region should be regarded as upper limits.

The friction (or drag force) exerted by the electrons on the ion beam is able to change the ion beam velocity. When applying a voltage ramp on the electron cooler, the friction can introduce uncertainties in the energy scale for collision energies smaller than about 1 meV. The details of this correction have been given by De Witt *et al.* [39].

The very accurate new transformer used for ion current measurements reduces the error in the determination of R_b to 3%. The largest errors are the uncertainty in the length of the interaction region (6%) and the combined statistical error in the measurements using the scintillation and surface barrier detectors (6%). The error in the determination of the electron density n_e is estimated to be 3.5%, which leads to an error of 10% in the measured rate coefficient as given in Eq. (2).

III. RESULTS

A. Dissociative recombination cross section

Figure 5 gives the dissociative recombination rate coefficient as a function of electron energy for both rotationally cold H_3^+ and rotationally warm H_3^+. The cold ion spectrum was taken with the Berkeley supersonic jet ion source and corresponds to ions produced at a rotational temperature of ~30 K as determined by subsequent infrared absorption measurements. The hot ion spectrum was taken with the JIMIS hollow cathode source [28], and should have a rotational temperature of greater than 300 K, although it is difficult to say how much hotter it would be. Hot sources like the MINIS heated filament source, which have ion temperatures greater than 1000 K, produce DR spectra that are much smoother in the region from 0–0.3 eV than is observed in Fig. 5. Under particular conditions, a hint of the structure in this region appeared when using the JIMIS source [28]. For detuning energies E_d large compared with the electron energy spread (about 2 meV), we can determine the cross section from the measured rate coefficient α_{DR} [from Eq. (2)] using the relation

$$\sigma(E_d)=\frac{\alpha_{\mathrm{DR}}}{v_d}, \tag{4}$$

where v_d is the detuning velocity of the electrons with respect to the ions. For detuning energies lower than a few meV, the approximation used in Eq. (4) is no longer useful, and the electron-velocity distribution must be taken into ac-

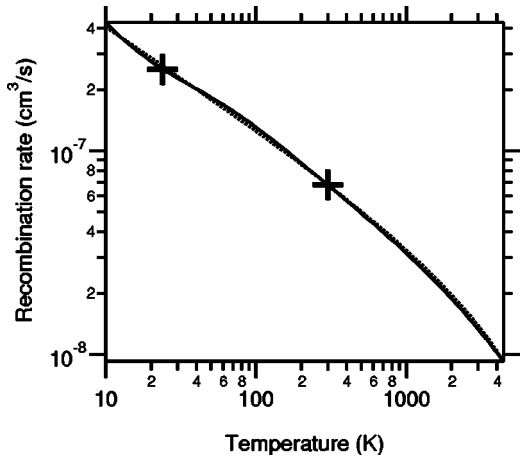

FIG. 6. Derived thermal rate coefficient as a function of electron temperature, for rotationally cold H_3^+ ions. Markers indicate 23 K (rotational temperature of H_3^+ towards ζ Persei) and 300 K. The dotted line is a power law fit [Eq. (7)].

count. The cross section can then be unfolded, using a numerical Fourier transform technique, from the exact relationship between rate coefficient and cross section

$$\alpha(v_d) = \int f(v_d,\vec{v})\sigma(v)v d^3\vec{v}, \tag{5}$$

where $\vec{v}$ is the relative velocity vector between an electron and an ion, v is the magnitude of this velocity vector, and the function $f(v_d,\vec{v})$ is the electron velocity distribution [40]. The experimentally determined cross section does not follow a $1/E^n$ dependence until below 0.1 meV, which makes it difficult to determine n with confidence because of the very few data points at these low energies. Our best estimate is that the cross section below about 0.1 meV can be described by the expression $\sigma(E)=3.1\times10^{-15}/E^{0.76}$ cm^3 s^{-1}, where E is in eV. The uncertainty in the transverse electron energy spread translates to a 25% uncertainty in the prefactor in this expression.

B. Thermal rate coefficient

For comparison to interstellar (as well as laboratory) DR processes, the quantity of interest is not exactly the DR rate at a specific electron energy, but the DR rate in the presence of a Maxwellian distribution of electron energies corresponding to the specified temperature (translational temperature of the interstellar medium). This can be calculated from the energy dependence of the cross section integrated over the electron distribution. The thermal rate coefficient, $\alpha(T_e)$, is given by

$$\alpha(T_e) = \frac{8\pi m_e}{(2\pi m_e kT_e)^{3/2}} \int \sigma(E) E e^{-E/kT_e} dE. \tag{6}$$

For the data collected using the Berkeley cold-ion source, the temperature dependence of the thermal rate coefficient is given in Fig. 6. These are the only data for the thermal DR rate coefficient for rotationally cold H_3^+ ions, and provide the best available values for calculating electron-ion recombination loss of H_3^+ in the interstellar medium. For the temperature of 23 K inferred from the spectrum of H_3^+ towards ζ Persei [31], we find $\alpha_{DR}=2.6\times10^{-7}$ cm^3 s^{-1}. For a room temperature electron distribution (but for rotationally cold ions), we find $\alpha_{DR}=6.8\times10^{-8}$ cm^3 s^{-1}. Over the range from 10–4000 K, the experimental thermal rate coefficient data are fit with a simple power law function (dotted line in Fig. 6), with the following form:

$$\alpha_{DR} = -1.3\times10^{-8} + 1.27\times10^{-6}T^{-0.48}, \tag{7}$$

which provides an analytical expression that agrees very well with the data.

The thermal rate coefficient was calculated using the low energy relationship $\sigma(E_d)=3.1\times10^{-15}/E_d^{0.76}$ cm^2 to extrapolate the cross section to 10^{-8} eV, which was used as the lower integration limit in Eq. (6). Adopting the theoretically expected $1/E$ dependence below 10^{-4} eV would lead to a substantial difference in the cross section, however, the thermal rate coefficient is virtually unaffected by this procedure (except for electron temperatures below 10 K). The uncertainty in the transverse electron energy spread introduces an uncertainty in the thermal rate coefficient of ~6% at 30 K and ~2% at 300 K.

C. Branching fractions

The branching fractions of the two possible break-up channels, H+H+H and H+H_2, were also investigated for the vibrationally and rotationally cold H_3^+ ions in the storage ring. The response of the SBD is not fast enough to distinguish between the product fragments from a given DR event, and thus all fragmented molecules are detected at the full beam energy. To study the branching fractions, a grid with known transmission $T=0.297$ [41] was placed in front of the SBD, and events were detected also at 1/3 and 2/3 of the full beam energy, corresponding to one and two hydrogen atoms. Together with the grid transmission T, the contribution to the three different peaks corresponding to the full beam energy and 2/3 and 1/3 of the full beam energy depends on the branching ratio between the two fragmentation channels H+H+H(N_α) and H+H_2(N_β), and this branching ratio was obtained by solving the system of linear equations

$$\begin{pmatrix} N_{3H} \\ N_{2H} \\ N_H \end{pmatrix} = \begin{pmatrix} T^3 & T^2 \\ 3T^2(1-T) & T(1-T) \\ 3T(1-T)^2 & T(1-T) \end{pmatrix} \begin{pmatrix} N_\alpha \\ N_\beta \end{pmatrix}, \tag{8}$$

where N_{3H}, N_{2H}, and N_H are the number of events detected at full beam energy, 2/3 of the beam energy, and 1/3 of the beam energy. This method is explained in more detail elsewhere [41].

Two separate measurements of the number of particles as a function of energy were performed with the grid in front of the SBD, one at a detuning energy of 0 eV and one at a detuning energy of 1.5 eV. The signal measured at 1.5 eV mainly originates from collisions with residual gas molecules, and represents the background contaminating the DR signal. The signal from the scintillation detector, which

monitors the beam intensity, was collected during both measurements and was used to scale the contribution of the background signal to the spectrum taken at 0 eV detuning energy. The background signal was subtracted before the contributions to the three separate energies were determined and the branching fractions calculated.

The resulting branching fractions were $N_\alpha = 64 \pm 5\%$ for the three body breakup and $N_\beta = 36 \pm 5\%$ for the two body break-up, where the error bars include the uncertainty in the grid transmission T as well as the statistical errors. This result differs slightly from the earlier measurements of Datz *et al.* [42], who measured the branching fractions as a function of detuning energy and found (at low energies) $N_\alpha = 75\%$ and $N_\beta = 25\%$. The latter experiment was performed with rotationally hot ions, so the discrepancy with the present experiment might be due to the difference in the average internal energy of the ions.

IV. DISCUSSION

A. Comparison with theory

For most ions, the dominant recombination mechanism is direct capture of an electron into a dissociative excited state of the neutral molecule, referred to as direct DR. The indirect mechanism involves a capture of the electron to a vibrationally excited Rydberg state, followed by predissociation of the Rydberg state by the same dissociative excited state that is involved in the direct mechanism. Theoretical values for the direct DR cross section determined by a time-dependent wave packet calculation agree very well with the observed DR cross sections at high electron energies (5–12 eV) for both H_3^+ and D_3^+ [43]. However, H_3^+—along with D_3^+, He_2^+, and HeH^+—is unusual in that, at low electron energies, direct DR processes do not significantly contribute to the recombination rate [44]. Consequently, for many years theoretical work [45] had supported very small recombination cross-sections owing to an absence of a suitable curve crossing between the H_3^+ electronic state in its ground vibrational level, and any energy level of neutral H_3.

This situation is illustrated in Fig. 7, which was adapted from Michels and Hobbs [45] and shows the energy levels corresponding to ground state $(^1A_1)H_3^+$, and the ground and excited states of neutral H_3. Various energy levels between the ground and excited states of H_3 have been omitted because they do not have curves that cross that of the H_3^+ state at reasonable energies. It can be seen that H_3^+ states with several quanta of vibrational excitation ($v \geq 3$) should have significantly better vibrational wavefunction overlap than those states with energies below the curve crossing. Owing to the difference in overlap at different vibrational levels, it had been suggested [14] that an abundance of vibrationally hot H_3^+ ions in the early DR measurements could reconcile the large observed recombination cross sections with the low values predicted by the direct DR mechanism.

In 1994, a new mechanism was proposed for such ions that lack a curve-crossing [46], and it was shown for HeH^+ that the indirect process dominates over the direct process. The success in explaining the DR of HeH^+ gave hope that a similar mechanism would drive the DR of H_3^+. When indirect DR mechanisms were accounted for by using a combined time-dependent wave packet multichannel quantum defect theory (MQDT) in two dimensions, the predicted cross section for H_3^+ DR increased by two orders of magnitude on average across the electron energy range 0–1 eV [44]. While this represented a significant step in the right direction, the theoretical predictions were still some three orders of magnitude lower than storage ring experiments.

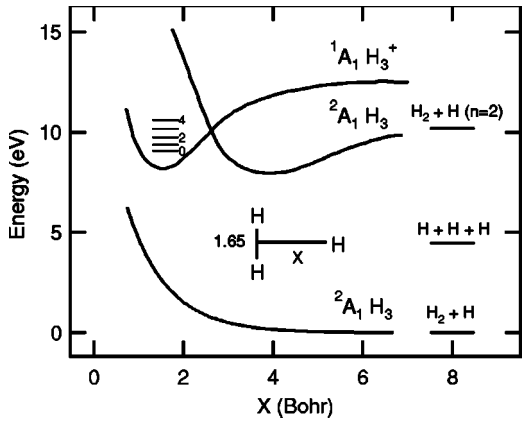

FIG. 7. Energy level diagram for H_3^+ and H_3 (adapted from [45]). The energy, relative to $H_2[^1\Sigma_g^+] + H[n=1]$, is shown as a function of the distance between the H_2 subunit (with $r_e = 1.65a_0 = 0.873$ Å for H_3^+) and H, for a C_{2v} symmetry structure. H_3 states that do not cross the H_3^+ surface are omitted, with the exception of the dissociative ground state. The energy levels of possible products are shown on the right.

In 2001, Kokoouline, Greene, and Esry [47] began a new theoretical treatment by developing a methodology to treat DR of H_3^+ in a full three-dimensional framework via MQDT and include Jahn-Teller distortion of the ion due to the field of the incoming electron. Their preliminary calculations did not include the branching ratios of predissociation and autoionization of the Rydberg state intermediates, and therefore provided upper and lower bounds to the H_3^+ DR rate, 3.4×10^{-10} cm^3 s$^{-1} < \alpha_{DR}(300\ \mathrm{K}) < 1.2 \times 10^{-8}$ cm^3 s^{-1}. The lower limit assumes that an electron captured into a Rydberg state always autoionizes back to the continuum, whereas the upper limit is obtained when autoionization does not occur and the Rydberg state is always predissociated. This represented the first time that DR calculations were within even an order of magnitude of storage ring measurements.

Around the time of the present experiments, Kokoouline and Greene [48,49] extended their calculations to a complete calculation of the DR rate for each individual rotational state. They also discovered that their earlier calculations were too low by a factor of π^2, owing to a "previously unrecognized inconsistency" in two different K-matrix conventions. Their calculations show significant structure in the low energy region (<1 eV) and a strong dependence of the magnitude of this structure on the rotational temperature, as is observed experimentally. Qualitatively, the observed structure is due to resonances where the energy of the electron nears the energy difference between the free ion and the neutral H_3 recombination intermediate. Since such resonances are a function of

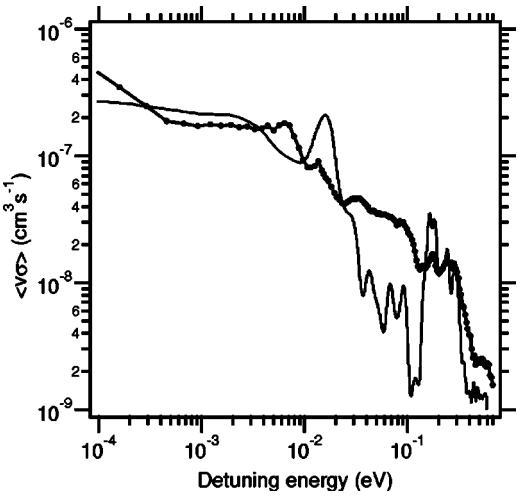

FIG. 8. Comparison between the measured dissociative recombination cross section (curve with dots, obtained using the Berkeley source), and theoretical calculations (grey curve) by Kokoouline and Greene [49]. See text for details.

the rotational state of the ion, a distribution of ions over many rotational states serves to "wash out" the overall structure because each rotational state has different resonances. Hence, our observation of structure in the DR rate represents additional evidence that the ions used in the present experiment were rotationally colder than those used in previous storage ring experiments.

Figure 8 shows a comparison of the measured energy dependence of the DR rate coefficient as given in Eq. (2) with the theoretical results of Kokoouline and Greene [49] for a low rotational temperature (40 K). The theoretical cross section shown in the figure [provided by Kokoouline and Greene (private communication)] was folded with an electron energy distribution, $f(v_d,\vec{v})$, according to Eq. (5), using a 2 meV transverse spread and a 0.1 meV longitudinal spread (i.e., the same conditions as the CRYRING experiment). Experimentally, the observed structure is less pronounced than that predicted by theory, which Kokoouline and Greene [49] suggest may be due to a small population of rotationally excited ions in the CRYRING experiment. But also for an ion such as HD^+, which has a dipole moment that drives the rotational population in a storage ring towards 300 K, theory predicts more pronounced resonances than actually measured [50]. It is interesting to note that theory and experiment agree better for H_3^+ than for HD^+ in the region below 20 meV.

As expected, in both the experimental case (see Fig. 5) and the theoretical case [49], the cross-section curve shows less structure at higher temperature than at lower temperature. At very low energies, the theoretical cross section [51] varies as $1/E$, which is expected from the Wigner threshold law [52,53]. The difference between the experimentally measured dependence on E and the theoretically predicted one is probably due to the difficulty in accurately measuring the cross section at very low energies. However, this difficulty has only minor impact on the derived thermal rate coefficients for reasonable temperatures, as the population of electrons at such low energies is small. For example, the difference between $1/E$ and $1/E^{0.76}$ extrapolations at low energy yields a difference in the derived thermal rate coefficient of only about 4% at 40 K and about 1% at 300 K.

Greene and Kokoouline [54] have made a comparison of their theoretical calculations and our experimental results in the "valley" region between 0.5–5 eV, where the toroidal correction described in Sec. II C must be applied to the experimental data. However, with the theoretical cross section available, Greene and Kokoouline were able to simulate the effect of the toroidal region on the measured rate, and then to compare this result with the experimental rate. The agreement was excellent, and this method avoids the difficulties of taking the difference of two large quantities, as discussed in Sec. II C.

For an electron distribution at 23 K and an ion rotational temperature of 40 K, Kokoouline and Greene calculate a value of $\alpha_{MQDT}(23\ \mathrm{K}) = 2.2\times10^{-7}\ \mathrm{cm}^3\ \mathrm{s}^{-1}$, which compares very favorably to the value determined from storage ring measurements using rotationally cold H_3^+ ions, $\alpha_{CRYRING}(23\ \mathrm{K}) = 2.6\times10^{-7}\ \mathrm{cm}^3\ \mathrm{s}^{-1}$. This remarkable agreement between theory and experiment (recall that only three years ago the discrepancy was three orders of magnitude) instills some degree of confidence in the applicability of the present experiment to the interstellar medium. Comparison with theoretical calculations is essential in this regard, because of the unavoidable differences between the conditions in the storage ring (magnetic field $B\sim300$ G and electron number density $n_e\sim10^7\ \mathrm{cm}^{-3}$) and those of the diffuse interstellar medium ($B\sim\mu$G, $n_e\sim10^{-2}\ \mathrm{cm}^{-3}$).

One additional piece of evidence supporting the convergence of theory and experiment is the recent prediction of the DR rate for D_3^+ by Kokoouline and Greene [49], which agrees with previous CRYRING experiments [55]. This means that there is agreement between the CRYRING experiments and theory concerning the isotope influence on the DR process.

B. Vibrational and rotational distribution of ions

Supersonic expansion sources generally provide better cooling of rotational energy than of vibrational energy, because of the greater efficiency of rotational-translational energy transfer relative to vibrational-translational transfer. In the presence of a discharge, one might expect the vibrational temperature of ions to be quite a bit higher than the rotational temperature, leading to the production of a small (but nonnegligible) population of vibrationally excited ions. This effect may, however, be mitigated to some extent by the high number density in the expansion and the large cross-section of ion-neutral collisions; for example, in Jupiter's ionosphere, H_3^+ is observed to have similar rotational and vibrational temperatures [56].

Nevertheless, we cannot rule out the possibility that our source produces some vibrationally excited ions. At reasonable vibrational temperatures, we may expect a small initial population in the $v_1=1$ (symmetric stretching mode) and $v_2=1$ (degenerate bending/stretching mode) states. The $v_2=1$ ions will relax to the vibrational ground state by spontaneous emission, on a timescale of several milliseconds (Einstein

coefficient $A=128.8\ s^{-1}$). Although the ν_1 mode is infrared inactive, and therefore relaxation from $v_1=1\rightarrow 0$ is forbidden, the transition $\nu_1\rightarrow\nu_2$ is allowed, although weak (and the $v_2=1$ ions can then quickly relax to the ground state). Dinelli *et al.* [57,58] have calculated the relaxation time of $\tau=1.2$ s for this process, and this relaxation pathway (and its timescale) have been experimentally verified by storage ring measurements at the Test Storage Ring [26]. Thus, we can conclude that all of the H_3^+ ions will relax into the vibrational ground state within a few seconds (all of our measurements were conducted after at least 4 seconds of storage).

Rotational cooling (or heating) in the storage ring by spontaneous emission (or absorption of blackbody photons) will not be important on the timescales of the experiment, because of the lack of a permanent dipole moment in the equilateral triangle-shaped H_3^+. A small dipole is, in fact, introduced by centrifugal distortion, but such "forbidden" rotational transitions are still very slow; for example, the lowest excited rotational level, (2, 2), radiatively relaxes to the (1,1) state with a lifetime of $\sim$27.2 days, given the Einstein coefficient given in Table 7 of Lindsay and McCall [34]. Hence, we expect that the rotational distribution produced by the ion source will remain unchanged throughout the experiment, unless changed by other mechanisms. Conceivable mechanisms include (1) relaxation of vibrationally excited ions, (2) heating during ion extraction from the source, (3) electron-impact excitation in the electron cooler, either in the straight section or in the toroidal regions. Because our conclusions depend on the assumption that the DR measurements were performed on rotationally cold ions, we examine each of these potential heating mechanisms in detail.

1. Relaxation of vibrationally excited ions

The "vibrational cascade" of vibrationally excited ions can lead to the production of rotationally excited ions in the vibrational ground state; however, this effect should be small. Because of the efficiency of rotational cooling in the supersonic expansion, even the vibrationally excited ions should be rotationally cold. The $v_2=1$ ions will be primarily in the $(J,G)=(0,1)$ level, which can only decay to (1,1) in the vibrational ground state because of the selection rules, and in the (1,2) level, which can only decay into (2,2). The $v_1=1$ ions will be in both the (1,0) and (1,1) levels. The $v_1=1$ (1,0) level can decay to (1,0) or (2,0) in $v_2=1$, which will then decay into (1,0) and (1,0) or (3,0) in the ground state. The $v_1=1$ (1,1) level can decay to (2,1), (1,1), or (0,1) in $v_2=1$, which will decay into (3,1), (2,1), and (1,1) in the ground state. Thus, the vibrationally excited ions can contribute somewhat to rotational excitation, but we expect this to be a minor effect (for $T_{vib}=1000$ K, only $<1\%$ of ions would be in $v_1=1$, and $<3\%$ of ions would be in $v_2=1$).

2. Extraction from source

Another possible heating source is during the interaction of the expansion with the skimmer, or during the extraction of the ions from the expansion. It is very difficult to quantitatively estimate the magnitude of such an effect, but we do not expect it to be a problem in our setup. However, before installing the skimmer we performed a set of DR measurements. In this skimmer-less configuration, we observed a great deal of arcing between the ion source and the first extraction optic on the endstation (between which there is a 30 kV potential drop); this problem is what led us to the use of a skimmer. Nevertheless, we were able to obtain some cross-section data (at a much lower signal to noise ratio). Qualitatively, we did not observe a significant difference between the experiments with and without the skimmer. However, when the backing pressure of the ion source was too low, and hence the cooling of the supersonic expansion inefficient, we did observe a qualitative change in the cross section. Without the skimmer in place, the ions experience the field of the 30 kV potential drop as soon as they are created; with the (grounded) skimmer in place, the ions are shielded from the 30 kV potential and experience only the ~ -800 V from the discharge electrode. It seems unlikely that both of these (very different) configurations could lead to the same degree of rotational excitation, which would argue that heating during the extraction is not significant. However, this heating source cannot be definitively ruled out without performing spectroscopy on the ions after the skimmer. However, due to the much lower number densities following the skimmer, this would require significantly more sensitive spectroscopic techniques than those employed here.

3. Excitation in the electron cooler

During the course of the ramping of the cathode voltage in the electron cooler (to measure the DR cross section), the stored H_3^+ ions will interact with electrons of various relative energies, which could induce rotational excitation by electron impact. For the lowest rotational levels in question, there are only three electron impact induced transitions that have reasonable cross sections, namely $(3,0)\leftarrow(1,0)$, $(2,1)\leftarrow(1,1)$, and $(3,1)\leftarrow(1,1)$. The cross sections for these transitions, as a function of electron impact energy, have recently been calculated by Faure and Tennyson [59]. By integrating these cross sections across the electron impact energies experienced during a 1.5 second ramping of the cathode voltage from detuning energies of 1 to 0 eV [as in the case of Fig. 4(b)], and considering the known number density of electrons in the electron cooler ($6.3\times10^6\ cm^{-3}$), we estimate that the probability for electron impact excitation of $(2,1)\leftarrow(1,1)$ is approximately 2.2%, and that for $(3,0)\leftarrow(1,0)$ is approximately 2.0%. To experimentally determine the effect of this heating on the measured DR cross section, we also performed DR measurements using ramps that only included energies below 20 meV and below 50 meV [see Fig. 4(d)] in order to stay below the thresholds of the $(2,1)\leftarrow(1,1)$ and $(3,0)\leftarrow(1,0)$ transitions, respectively. The DR cross sections measured in these experiments overlapped with the cross sections measured using the full ramp, which implies that this heating is not affecting our results. As an additional test, we performed an experiment where the electron cooler was held at 64 meV [just above the $(3,0)\leftarrow(1,0)$ threshold] for 1.5 seconds, and then the DR cross section was measured. Under these conditions, given the electron impact cross sections of Faure and Tennyson, we would expect approximately 4.5% of the (1,1) ions to be-

come excited to (2,1), and 2.4% of the (1,0) ions to be excited to (3,0); again, we saw no change in the measured DR cross section.

We also performed branching fraction measurements (as described in Sec. III C) following 1 second of "heating" at 60 mV detuning energy. This measurement yielded $N_\alpha = 66 \pm 5\%$ and $N_\beta = 34 \pm 5\%$, only slightly different from the result without "heating," and identical within the uncertainties. This may constitute additional evidence that the ions are not efficiently heated in the electron cooler, as the experiments of Datz *et al.* [42] found $N_\alpha = 75\%$ for rotationally hot ions.

Electron impact excitation may also occur in the toroidal regions of the electron cooler, where the H_3^+ ions are constantly exposed to high energy electrons, even when the cathode voltage is set for maximum cooling. Combining the known electron energy as a function of position in the electron cooler and the electron impact cross sections from Faure and Tennyson, we estimate that the probability of $(3,0) \leftarrow (1,0)$ excitation is 0.16% and that of $(2,1) \leftarrow (1,1)$ excitation is 0.17% per second of beam circulation. In a typical experiment where the beam is stored for a total of 8 seconds, we would then expect only ~1.3% of the ions to be rotationally excited by this mechanism. Some of this excitation may be offset by deexcitation in the straight section of the electron cooler when the cathode voltage is set for maximum cooling, but we have not attempted to estimate the magnitude of this mitigating effect.

V. CONCLUSIONS

Dissociative recombination rate measurements for a rotationally cold distribution of H_3^+ have been performed using the CRYRING ion storage ring at the Manne Siegbahn Laboratory at Stockholm University, Sweden. The supersonic expansion ion source was designed, built, and spectroscopically characterized at the University of California at Berkeley. The source design incorporated a ring-electrode dc discharge plasma and a pinhole, pulsed supersonic jet to maximize ion production while minimizing the temperature. Stable plasma conditions and high backing pressures of pure H_2 gas produced rotational state distributions that corresponded to rotational temperatures of ~30 K—nearly the same as the rotational state distribution observed in the diffuse interstellar cloud along the sightline towards the star ζ Persei (23 K). The populations of the two lowest allowed rotational quantum states were monitored as a function of source conditions by recording the absorption spectrum of the $R(1,0)$ and $R(1,1)^u$ transitions at 2725.9 cm^{-1} and 2726.2 cm^{-1}, respectively, and it was found that the ion source produced rotationally cold (~20–60 K) ions over a wide range of operating conditions.

The DR rate measured in these experiments (the first measurements of rotationally cold H_3^+ ions) is very similar to the theoretical predictions of Kokoouline and Greene. The low temperature of the ions resulted in the most distinct structure in the DR rate measured yet (see Fig. 5). While the magnitude of the resonances in the DR rate as a function of electron energy was less than that predicted by Kokoouline and Greene, the calculated and observed energy dependence both had qualitatively similar structure. As the H_3^+ ions used in the present experiment have a lower rotational temperature than those in previous experiments, our thermal DR rate coefficient represents the best available value for use in the modeling of the diffuse interstellar medium.

ACKNOWLEDGMENTS

The authors are thankful to the staff of the Manne Siegbahn Laboratory for help with the experiment. B.J.M. has been supported by the Miller Institute for Basic Research in Science. A.J.H. and R.J.S. acknowledge support from AFOSR Chemical Physics program and the National Science Foundation. N.D. and G.H.D. were supported in part by the U.S. Department of Energy, Office of Fusion Energy. J.S. is supported in part by the State Committee for Scientific Research Support. Support is acknowledged from the European Office of Aerospace Research and Development (EOARD), the Swedish Research Council, and the Swedish Foundation for International Cooperation in Research and Higher Education (STINT). This work was also supported by the European Community's Research Training Network Programme under Contract No. HPRN-CT-2000-0142 and Training Site Programme under Contract No. HPMT-CT-2001-0026.

[1] J. J. Thomson, Philos. Mag. **21**, 225 (1911).
[2] A. J. Dempster, Philos. Mag. **31**, 438 (1916).
[3] T. R. Hogness and E. G. Lunn, Phys. Rev. **26**, 44 (1925).
[4] H. Eyring, J. O. Hirschfelder, and H. S. Taylor, J. Chem. Phys. **4**, 479 (1936).
[5] J. O. Hirschfelder, J. Chem. Phys. **6**, 795 (1938).
[6] D. W. Martin, E. W. McDaniel, and M. L. Meeks, Astrophys. J. **134**, 1012 (1961).
[7] W. D. Watson, Astrophys. J. Lett. **183**, L17 (1973).
[8] E. Herbst and W. Klemperer, Astrophys. J. **185**, 505 (1973).
[9] T. R. Geballe and T. Oka, Nature (London) **384**, 334 (1996).
[10] B. J. McCall, T. R. Geballe, K. H. Hinkle, and T. Oka, Astrophys. J. **522**, 338 (1999).
[11] B. J. McCall, T. R. Geballe, K. H. Hinkle, and T. Oka, Science **279**, 1910 (1998).
[12] B. J. McCall, K. H. Hinkle, T. R. Geballe, G. H. Moriarty-Schieven, N. J. Evans, K. Kawaguchi, S. Takano, V. V. Smith, and T. Oka, Astrophys. J. **567**, 391 (2002).
[13] T. Oka, in *Dissociative Recombination of Molecular Ions with Electrons*, edited by S. L. Guberman (Kluwer, New York, 2003), pp. 209–220.
[14] M. Larsson, Philos. Trans. R. Soc. London, Ser. A **358**, 2433 (2000).
[15] R. Plašil, J. Glosík, V. Poterya, P. Kudrna, J. Rusz, M. Tichý, and A. Pysanenko, Int. J. Mass. Spectrom. **218**, 105 (2002).
[16] M. T. Leu, M. A. Biondi, and R. Johnsen, Phys. Rev. A **8**, 413

(1973).
[17] D. Smith and N. G. Adams, Astrophys. J. Lett. **284**, L13 (1984).
[18] N. G. Adams and D. Smith, in *Dissociative Recombination: Theory, Experiment, and Applications*, edited by J. B. A. Mitchell and S. L. Guberman (World Scientific, Singapore, 1989), pp. 124–140.
[19] E. F. van Dishoeck and J. H. Black, Astrophys. J., Suppl. Ser. **62**, 109 (1986).
[20] T. Amano, Astrophys. J. Lett. **329**, L121 (1988).
[21] T. Amano, J. Chem. Phys. **92**, 6492 (1990).
[22] G. Sundström *et al.*, Science **263**, 785 (1994).
[23] T. Tanabe *et al.*, in *Dissociative Recombination: Theory, Experiment and Applications, Vol. IV*, edited by M. Larsson, J. B. A. Mitchell, and I. F. Schneider (World Scientific, Singapore, 2000), pp. 170–179.
[24] M. J. Jensen, H. B. Pedersen, C. P. Safvan, K. Seiersen, X. Urbain, and L. H. Andersen, Phys. Rev. A **63**, 052701 (2001).
[25] J. Glosík, R. Plašil, V. Poterya, P. Kudrna, and M. Tichý, Chem. Phys. Lett. **331**, 209 (2000).
[26] H. Kreckel *et al.*, Phys. Rev. A **66**, 052509 (2002).
[27] D. Strasser, L. Lammich, H. Kreckel, S. Krohn, M. Lange, A. Naaman, D. Schwalm, A. Wolf, and D. Zajfman, Phys. Rev. A **66**, 032719 (2002).
[28] M. Larsson, N. Djuric, G. H. Dunn, A. Neau, A. M. Derkatch, F. Hellberg, S. Kalhori, D. B. Popovic, J. Semaniak, Å. Larson, and R. Thomas, in *Dissociative Recombination of Molecular Ions with Electrons*, edited by S. L. Guberman (Kluwer, New York, 2003), pp. 87–94.
[29] L. Lammich, D. Strasser, H. Kreckel, M. Lange, H. B. Pedersen, S. Altevogt, V. Andrianarijaona, H. Buhr, O. Heber, P. Witte, D. Schwalm, A. Wolf, and D. Zajfman, Phys. Rev. Lett. **91**, 143201 (2003).
[30] A. Wolf, L. Lammich, D. Strasser, S. Altevogt, V. Andrianarijaona, H. Buhr, O. Heber, H. Kreckel, H. B. Pedersen, D. Schwalm, and D. Zajfman, Phys. Scr., T **110**, 193 (2004).
[31] B. J. McCall, A. J. Huneycutt, R. J. Saykally, T. R. Geballe, N. Djuric, G. H. Dunn, J. Semaniak, O. Novotny, A. Al-Khalili, A. Ehlerding, F. Hellberg, S. Kalhori, A. Neau, R. Thomas, F. Österdahl, and M. Larsson, Nature (London) **422**, 500 (2003).
[32] A. J. Huneycutt, R. J. Stickland, F. Hellberg, and R. J. Saykally, J. Chem. Phys. **118**, 1221 (2003).
[33] J. B. Paul, C. P. Collier, R. J. Saykally, J. J. Scherer, and A. O'Keefe, J. Phys. Chem. A **101**, 5211 (1997).
[34] C. M. Lindsay and B. J. McCall, J. Mol. Spectrosc. **210**, 60 (2001).
[35] A. Neau, Ph.D. thesis, Stockholm University, 2002.
[36] A. Le Padellec, N. Djuric, A. Al-Khalili, H. Danared, A. M. Derkatch, A. Neau, D. B. Popovic, S. Rosén, J. Semaniak, R. Thomas, M. af Ugglas, W. Zong, and M. Larsson, Phys. Rev. A **64**, 012702 (2001).
[37] A. Paal, A. Simonsson, A. Källberg, J. Dietrich, and I. Mohos, in DIPAC 2003 Proceedings, Mainz, Germany, 2004, p. 240, http://bel.gsi.de/dipac2003
[38] A. Lampert, A. Wolf, D. Habs, J. Kenntner, G. Kilgus, D. Schwalm, M. Pindzola, and N. Badnell, Phys. Rev. A **53**, 1413 (1996).
[39] D. R. DeWitt, R. Schuch, H. Gao, W. Zong, S. Asp, C. Biedermann, M. H. Chen, and N. R. Badnell, Phys. Rev. A **53**, 2327 (1996).
[40] C. Strömholm, J. Semaniak, S. Rosén, H. Danared, S. Datz, W. van der Zande, and M. Larsson, Phys. Rev. A **54**, 3086 (1996).
[41] A. Neau, A. A. Khalili, S. Rosén, A. Le Padellec, A. M. Derkatch, W. Shi, L. Vikor, M. Larsson, J. Semaniak, R. Thomas, M. B. Någård, K. Andersson, H. Danared, and M. af Ugglas, J. Chem. Phys. **113**, 1762 (2000).
[42] S. Datz, G. Sundström, C. Biedermann, L. Broström, H. Danared, S. Mannervik, J. R. Mowat, and M. Larsson, Phys. Rev. Lett. **74**, 896 (1995).
[43] A. E. Orel, I. F. Schneider, and A. Suzor-Weiner, Philos. Trans. R. Soc. London, Ser. A **358**, 2445 (2000).
[44] I. F. Schneider, A. E. Orel, and A. Suzor-Weiner, Phys. Rev. Lett. **85**, 3785 (2000).
[45] H. H. Michels and R. H. Hobbs, Astrophys. J. Lett. **286**, L27 (1984).
[46] S. L. Guberman, Phys. Rev. A **49**, R4277 (1994).
[47] V. Kokoouline, C. H. Greene, and B. D. Esry, Nature (London) **412**, 891 (2001).
[48] V. Kokoouline and C. H. Greene, Phys. Rev. Lett. **90**, 133201 (2003).
[49] V. Kokoouline and C. H. Greene, Phys. Rev. A **68**, 012703 (2003).
[50] I. F. Schneider, C. Strömholm, L. Carata, X. Urbain, M. Larsson, and A. Suzor-Weiner, J. Phys. B **30**, 2687 (1997).
[51] V. Kokoouline (private communication).
[52] E. P. Wigner, Phys. Rev. **73**, 1002 (1948).
[53] A. R. P. Rau, Comments At. Mol. Phys. **14**, 285 (1984).
[54] C. H. Greene and V. Kokoouline, Phys. Scr., T **110**, 178 (2004).
[55] M. Larsson, H. Danared, Å. Larson, A. Le Padellec, J. R. Peterson, S. Rosen, J. Semaniak, and C. Strömholm, Phys. Rev. Lett. **79**, 395 (1997).
[56] S. Miller, R. D. Joseph, and J. Tennyson, Astrophys. J. Lett. **360**, L55 (1990).
[57] B. M. Dinelli, S. Miller, and J. Tennyson, J. Mol. Spectrosc. **153**, 718 (1992).
[58] B. M. Dinelli, S. Miller, and J. Tennyson, J. Mol. Spectrosc. **156**, E243 (1992).
[59] A. Faure and J. Tennyson, J. Phys. B **35**, 3945 (2002).